Open Access Full Text Article

ORIGINAL RESEARCH

Analysis of the Value of Quantitative Features in Multimodal MRI Images to Construct a Radio-Omics Model for Breast Cancer Diagnosis

Zhitao Zhang, Huan Lan, Shuai Zhao

Department of Galactophore, Fujian Maternity and Child Health Hospital, Fuzhou, Fujian Province, 350001, People's Republic of China

Correspondence: Shuai Zhao, Department of Galactophore, Fujian Maternity and Child Health Hospital, No. 18 Daoshan Road, Gulou District, Fuzhou City, Fujian Province, 350001, People's Republic of China, Email zhaoshuaizh@21cn.com

Objective: To analyze the diagnostic value of quantitative features in multimodal magnetic resonance imaging (MRI) images to construct a radio-omics model for breast cancer.

Methods: Ninety-five patients with breast-related diseases from January 2020 to January 2021 were grouped into the benign group (n=57) and malignant group (n=38) according to the pathological findings. All cases were randomized as the training group (n=66) and validation group (n=29) in a 7:3 ratio based on the examination time. All subjects were examined by T1-weighted imaging (T1WI), T2-weighted imaging (T2WI), diffusion-weighted imaging (DWI), dynamic contrast enhancement (DCE), and apparent diffusion coefficient (ADC) multimodality MRI. The MRI findings were analyzed against pathological findings. A diagnostic breast cancer radiomics model was constructed. The diagnostic efficacy of the model in the validation group was analyzed, and the diagnostic efficacy was analyzed via the ROC curve.

Results: Fibroadenoma accounted for 49.12% of benign breast diseases, and invasive ductal carcinoma accounted for 73.68% of malignant breast diseases. The sensitivity of T1WI, T2WI, DWI, ADC, and DCE in diagnosing breast cancer was 61.14%, 66.67%, 73.30%, 78.95%, and 85.96%, using the four-fold table method. The area under the curves (AUCs) of T1WI, T2WI, DWI, ADC, and DCE for diagnosing breast cancer were 0.715, 0.769, 0.785, 0.835, and 0.792, respectively. The AUCs of plain scan, diffuse, enhanced, plain scan + diffuse, plain scan + enhanced, enhanced + diffuse, and plain scan + enhanced + diffuse for diagnosing breast cancer were 0.746, 0.798, 0.816, 0.839, 0.890, 0.906, and 0.927, respectively.

Conclusion: The construction of a radio-omics model by quantitative features in multimodal MRI images was valuable in the diagnosis of breast cancer. The value of radio-omics models such as plain scan + enhanced + diffuse was higher than the other models in diagnosing breast cancer and could be widely applied in clinical practice.

Keywords: MRI, quantitative features, imaging histology, model, breast cancer, diagnosis

Introduction

Breast cancer is a major health concern for women due to its high mortality and morbidity, and its 5-year survival rate is less than 30% even with adjuvant chemotherapy for metastatic breast cancer.[1,2] According to the International Agency for Research on Cancer, breast cancer is the most common cancer among women and the leading cause of cancer death, followed by colorectal cancer and lung cancer. In China, the incidence rate of breast cancer is the highest among female malignant tumors. With the increase in life pressure and the acceleration of life rhythm in recent years, the incidence rate of breast cancer has increased year by year, which has a great impact on women's physical and mental health and quality of life. It has become the focus of medical research worldwide. Early diagnosis and early treatment are of great significance to improve the treatment effect and prognosis of breast cancer.[3,4] There are many imaging methods for the examination and diagnosis of breast diseases, including breast ultrasound, mammography, and magnetic resonance imaging (MRI) examination. Among them, contrast-enhanced T1-weighted imaging (T1WI) and T2-weighted imaging (T2WI) are MRI routine scan sequences. T1WI refers to the height of tissue signal intensity in the magnetic resonance

image reflecting the difference in tissue longitudinal relaxation, and T2WI is the basis of other scan sequences conduciveness to observing lesions. Both T1WI and T2WI have certain value in diagnosing breast cancer. Diffusion-weighted imaging (DWI) is used to evaluate the effect of radiotherapy and chemotherapy for breast cancer by analyzing the changes of micro diffusion of water inside and outside cells to check the functional environment of tissues and the physiological information of water molecule movement.[5] Apparent diffusion coefficient (ADC) is used to describe the speed and range of diffusion movement of molecules in different directions in DWI sequences, and is the most commonly used and basic indicator of MRI DWI, which can more accurately reflect the heterogeneity of tumor tissue and provide more accurate and reliable diagnostic results.[6] Dynamic contrast enhancement (DCE) can be used to analyze tissue vascular density and has a high value in detecting sensitivity of tumor vascular density changes and evaluating lymph node metastasis of breast cancer.[7] In recent years, with the rapid development of medical imaging technology and the proficient application of artificial intelligence, radio-omics has become a new method of medical diagnosis, the main content of which is to obtain quantitative features from standard medical images in high throughput, convert the images into a mineable data space, and then analyze these data for decision support. In this way, it is expected that imaging big data will be used to formulate cancer diagnosis and treatment plans, which not only provides an objective method for assessing tumor heterogeneity, but also adds a new dimension to precision medicine.[8] Radio-omics is mainly used in the imaging of head, neck, and lung diseases. Moreover, some studies believe that the radio-omics model may be helpful in the accurate diagnosis of breast cancer.[9]

In this study, 95 patients with breast-related diseases were picked to analyze the diagnostic value of radio-omics model constructed based on quantitative features in MRI images for breast cancer.
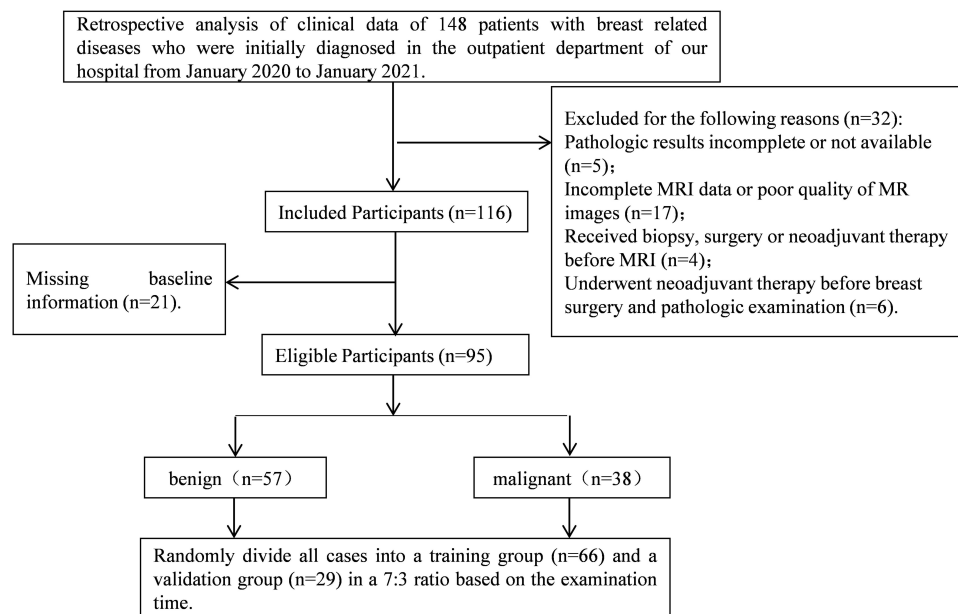
Materials and Methods

General Materials

The clinical data of 95 patients with breast-related diseases who received an initial diagnosis in our hospital from January 2020 to January 2021 were retrospectively analyzed. Inclusion criteria: (1) Patients aged 25–80 years old. (2) All patients were confirmed as having breast cancer by ultrasound examination, molybdenum target screening, and MRI examination. (3) Lesions were diagnosed as benign and malignant by biopsy or surgical resection. (4) The patient and their family members are informed and have good compliance. They could cooperate with the examination and treatment, and all signed the informed consent forms. Exclusion criteria: (1) Patients with other malignant tumors. (2) Patients with incomplete clinical data. (3) Patients with unclear MRI images. All patients were grouped into a benign group (n=57) and a malignant group (n=38) based on pathological results. All experimental operations were ratified by the hospital Ethics Committee and complied with the Declaration of Helsinki. The general information selection process is shown in Figure 1.

Methods

Siemens MRI breast scanner Magnetom Espree Pink and 16-channel dual breast surface dedicated coil were used. The patient was instructed to lie prone on the examination table, raise their hands to the head, and place their breasts naturally suspended in the coil. Multimodal MRI examinations such as T1WI, T2WI, DWI, ADC, and DCE were performed sequentially. (1) T1WI parameters: horizontal axis position, 2.46ms TE, 6.00ms TR, 1.6.00mm layer thickness and 360 × 360mm FOV. (2) T2WI parameters: horizontal axis position, 54.00ms TE, 4000ms TR, 4.00mm layer thickness, and 340 × 340mm FOV. (3) DWI parameters: horizontal axis position, 50.00ms TE, 5500ms TR, 5.00mm layer thickness, 280 × 280mm. The diffusion sensitivity factors b of FOV are 50, 400, and 800s^2/mm, respectively. Gd-DTPA contrast agent was injected at 2.5mL/s for 10 seconds. ADC diagrams were automatically generated by Siemens workstations. (4) DCE parameters: 3D fast gradient echo sequence, 4.00ms TE, 7.50ms TR, 2.00mm layer thickness. The transverse section was scanned 9 consecutive times for 8 minutes. Multi-modal MRI images were pretreated, and Region of Interest (ROI) was selected to extract quantitative features of radio-omics. Complete MRI images of all enrolled patients were collected, and the mammary gland of the DCE-MRI image was segmented layer by layer with the region of interest, that was, 3D segmentation, which could fully reflect the overall situation of the tumor and expose complete tumor information. Image

Retrospective analysis of clinical data of 148 patients with breast related diseases who were initially diagnosed in the outpatient department of our hospital from January 2020 to January 2021.

Excluded for the following reasons (n=32):
Pathologic results incompplete or not available (n=5)；
Incomplete MRI data or poor quality of MR images (n=17)；
Received biopsy, surgery or neoadjuvant therapy before MRI (n=4)；
Underwent neoadjuvant therapy before breast surgery and pathologic examination (n=6).

Included Participants (n=116)

Missing baseline information (n=21).

Eligible Participants (n=95)

benign（n=57）

malignant（n=38）

Randomly divide all cases into a training group (n=66) and a validation group (n=29) in a 7:3 ratio based on the examination time.

**Figure I** The selection process of general information.

analysis and measurement were carried out independently by two doctors of different seniority at the post-processing workstation. T2WI and DCE-MRI images were also used for delineation. When sketching ROI, first perform ROI delineation on DWI, then copy the ROI to the ADC plot to outline the lesion, and measure the corresponding ADC value. The measurement method: The small ROI method measured the ADC value: The ROI size was about $0.07cm^2$, two small circles were drawn as regions of interest in the largest area of the tumor to measure the ADC, and the average value of the two was taken as the measurement value after avoiding necrosis, cystic changes, bleeding and other areas. The area ROI method measured the ADC value: The area at the largest level of the tumor was delineated as an ROI measurement ADC, avoiding the cystic lesion and necrosis area visible to the naked eye. The volumetric ROI method measured the ADC value: The area of each layer of the tumor was delineated as the ROI measurement ADC, and the average ADC value of all the contoured layers of the tumor was taken as the measurement value. The ADC values measured by the two observers were averaged as the final measurement. The quantitative features of radio-omics were extracted, and plain scan (T1WI, T2WI), diffusion (DWI, ADC), enhanced (DCE) and other MRI examinations extracted from the ROI region of lesions were used to extract morphological features, first-order features, and texture features. The representative features with the highest discriminative power were selected and applied to construct a radio-omics model using Support Vector Machines (SVM):[10] SVM was a binary classification model in which SVM constructed a hyperplane so that the edges of two classes in a high-dimensional feature space were spaced at the maximum, and the vector that defined the hyperplane was called a support vector. Use the "e1071" package of R software to build the model, download the support vector machine package, import data, divide the data, use 2/3 of the data as the training set with 1/3 of the data as the verification set, build the model with the model prediction, and calculate the accuracy of the model prediction and other indicators.

Feature selection: After selecting image group features, the Spearman correlation test is used for feature simplification to avoid overfitting. Spearman correlation analysis performed feature preprocessing, and texture parameters with correlation coefficient higher than 0.9(| r |>0.9) were removed to obtain the final feature parameters. The representative feature with the highest discrimination (AUC value) in each group is selected, and other features are deleted. Then, the LASSO algorithm is used to select key features with classification ability to establish a radio-omics model. The LASSO logistic regression model can reduce the dimensionality of high-dimensional data and screen out features with predictive value. In the feature selection process of the LASSO logistic regression model, the feature coefficients that do not have predictive value are reduced to zero, and these features are deleted. Then, other non-zero features are

selected for cross-validation analysis with ten folds. Finally, the optimal feature is determined by the optimal average AUC value of the LASSO logistic regression model performing tenfold cross-validation in the training group. Spearman correlation test and LASSO logistic regression analysis were conducted using MATLAB R2018b (MathWorks Inc.) software.

Model establishment:[11] The imaging omics features of T1WI, T2WI, DWI, ADC, and DCE quantitative parameter maps of all cases were evaluated. The consistency of lesion segmentation within and between observers was evaluated, and ICC>0.75 indicates good consistency. All cases were randomized as a training group (n=66) and a validation group (n=29) in a 7:3 ratio based on the examination time. The MRI images are shown in Figure 2. Then all T1WI, T2WI, DWI, ADC, DCE 5 sequences were combined as plain scan + enhanced group (T1WI+T2WI+DCEI), plain scan + diffuse group (T1WI+T2WI+DWI+ADC+ADC), enhanced + diffuse (DWI+ADC+DCE), and plain scan + enhanced + diffuse group (T1WI+T2WI+DWI+ADC+DCE).

The model is established using a Support Vector Machine (SVM) classifier. SVM Classifier was implemented using Toolkit libsvm-3.21 in MATLAB (https://www.csie.ntu.edu.tw/ ~Cjlin/ibsvm/). For the combination of two or three sequences, support vector machine models with key features are trained based on training groups. ROC curves were drawn in the validation group to evaluate the model. To evaluate the performance of the model, MathWorks R2018b (MathWorks Inc.) software was used to calculate the area under the curve (AUC), accuracy, sensitivity, and specificity.
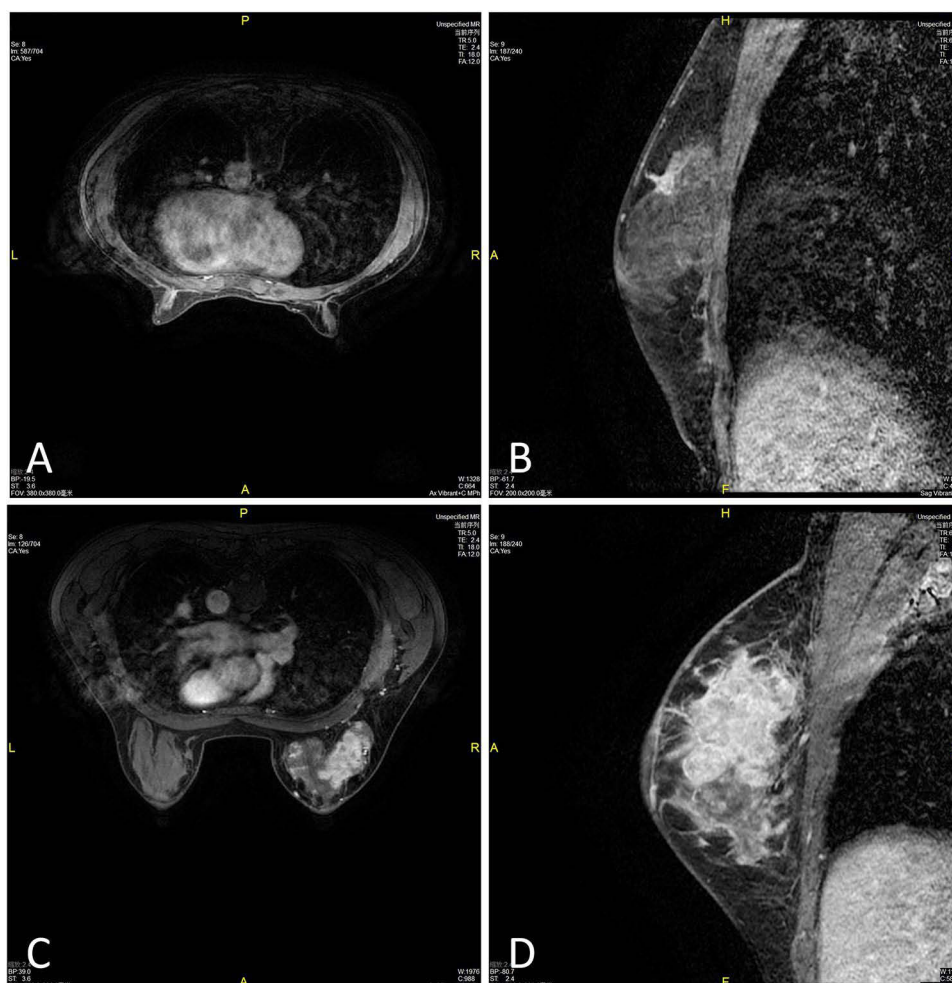
Figure 2 MRI images of the training and validation group.
Note: (**A** and **B**) was the training group, and (**C** and **D**) was the validation group.

Outcome Measures

Clinicopathological data: The clinical data of the patients in two groups were collected, including the age, BMI, tumor size, menstruation, ethnicity, human epidermal growth factor receptor 2 (HER2) status, education, marital status, smoking, drinking, age of first menstruation, delivery, breast cancer family history, etc. The disease types and proportions of two groups of patients were analyzed.

Comparative analysis of MRI and pathological results: The four-fold table method was used to analyze the differences between MRI and pathological results. Sensitivity=True Benign Number/(True Benign Number+False Malignant Number) * 100%, specificity=True Malignant Number/(True Malignant Number+False Benign Number) * 100%.

Statistical Analysis

The experimental data were analyzed using SPSS 20.0 software. Measurement data such as age, tumor size, and initial menstrual age were shown as $(\bar{x} \pm s)$ and compared using a t-test. Enumeration data such as disease type, menstrual status, and marital status were expressed in the form of (%) and compared using χ^2 or Fisher test. The statistically significant results were those with $P<0.05$. The receiver operating characteristic curve (ROC curve) was used to analyze the AUC, sensitivity, specificity, and accuracy thresholds of single and multi-radio-omics models.

Results

Comparison of General Information

In this experiment, 57 cases of benign breast diseases were diagnosed through pathological examination, with fibroadenoma accounting for the highest proportion (49.12%). Thirty-eight cases of malignant breast diseases were diagnosed, with invasive ductal carcinoma accounting for the highest proportion, accounting for 73.68%. In the malignant group, there were 25 cases of BI-RADS grade 4, 13 cases of BI-RADS grade 5, 19 cases of TNM grade I, 12 cases of grade II, and 7 cases of grade III. The age and tumor size of patients in the malignant group were significantly higher than those in the benign group ($P<0.05$, Tables 1 and 2).

Comparative Analysis of MRI Examination results and Pathological Results

Four-fold table analysis showed that the sensitivity and specificity of T1WI in the diagnosis of breast cancer were 61.14% and 73.68%, respectively; The sensitivity and specificity of T2WI in diagnosing breast cancer were 66.67% and 71.05%, respectively; The sensitivity and specificity of ADC in diagnosing breast cancer were 73.30% and 78.95%, respectively; The sensitivity and specificity of DCE in diagnosing breast cancer were 78.95% and 86.84%, respectively; The sensitivity and specificity of DWI in the diagnosis of breast cancer were 85.96% and 84.21% respectively (Table 3).

Extracting Radio-Omics Parameters Related to Lesions

According to the inclusion time, the cases were divided into a training group (n=66) and a validation group (n=29). No difference existed in age, BMI and tumor size between the two groups ($P>0.05$, Table 4). MRI examinations such as plain scan (T1WI, T2WI), diffusion (DWI, ADC), and enhancement (DCE) was extracted from the ROI area of the lesion

Table 1 Analysis of the Proportion of Disease Types (Cases, %)

Type of Lesion	The Benign Group		Type of Lesion	The malignant Group	
	Cases	%		Cases	%
Fibroadenoma	28	49.12	Infiltrating ductal carcinoma	28	73.68
Hyperplastic nodule	10	17.54	Mucinous carcinoma	1	2.63
Chronic inflammation of the breast	11	19.30	Mucinous carcinoma	2	5.26
Breast adenosis	6	10.53	Infiltrating papillary carcinoma	1	2.63
Intraductal papillary ovoma	3	5.26	Ductal carcinoma in situ	6	10.53
Total	57	100.00%	Total	38	100.00

Table 2 Comparison of General Information ($\bar{x} \pm s$)

Indicators		The Benign Group (n=57)	The Malignant Group (n=38)	t/χ²	P
Age		41.05±8.96	50.17±12.05	4.227	<0.001
BMI		22.36±1.58	23.01±2.05	1.741	0.084
Mass size		0.98±0.26	1.28±0.45	4.113	<0.001
Menstrual condition	menopause	18 (31.58%)	15 (39.47%)	0.628	0.428
	Premenopausal	39 (68.42%)	23 (60.53%)		
Ethnicity	Han	50 (87.72%)	35 (92.11%)	0.466	0.495
	Others	7 (12.28%)	3 (7.89%)		
HER2 state	Low HER2 expression	23 (40.35%)	15 (39.47%)	0.007	0.937
	HER2-0	34 (59.65%)	23 (60.53%)		
Education level	Primary school and below	19 (33.33%)	15 (39.47%)	0.521	0.770
	Middle school and vocational school	25 (43.86%)	14 (36.84%)		
	Bachelor's degree or above	13 (22.81%)	9 (23.68%)		
Marital status	First marriage	38 (66.67%)	26 (687.42%)	1.179	0.757
	remarriage	10 (17.54%)	4 (10.53%)		
	Divorce	5 (8.77%)	4 (10.53%)		
	Widow	4 (7.02%)	4 (10.53%)		
Smoking		14 (24.56%)	10 (26.32%)	0.037	0.847
Drinking		8 (14.04%)	5 (13.16%)	0.014	0.902
Age of initial menstrual period		12.96±2.15	13.52±1.46	1.403	0.163
Delivery situation	Yes	41 (71.93%)	30 (78.95%)	0.594	0.440
	No	16 (28.07%)	8 (21.05%)		
Family history of breast cancer		14 (24.56%)	12 (31.58%)	0.564	0.452

Table 3 Comparative Analysis of MRI Examination Results and Pathological Results (Cases, %)

Test Mode		Pathological Results		Total	Sensitivity	Specificity
		Benign	Malignancy			
T1WI	Benign	35 (36.84%)	10 (10.53%)	63 (66.32%)	61.14%	73.68%
	Malignancy	22 (23.16%)	28 (29.47%)	32 (33.68%)		
	Total	57 (60.00%)	38 (40.00%)	95 (100.00%)		
T2WI	Benign	38 (40.00%)	11 (11.58%)	65 (68.42%)	66.67%	71.05%
	Malignancy	19 (20.00%)	27 (28.42%)	30 (31.58%)		
	Total	57 (60.00%)	38 (40.00%)	95 (100.00%)		
ADC	Benign	41 (43.16%)	8 (8.42%)	71 (74.74%)	71.30%	78.95%
	Malignancy	16 (16.84%)	30 (31.58%)	24 (25.26%)		
	Total	57 (60.00%)	38 (40.00%)	95 (100.00%)		
DCE	Benign	45 (47.37%)	5 (5.26%)	78 (82.11%)	78.95%	86.84%
	Malignancy	12 (12.63%)	33 (34.74%)	17 (17.89%)		
	Total	57 (60.00%)	38 (40.00%)	95 (100.00%)		
DWI	Benign	49 (51.58%)	6 (6.31%)	81 (85.26%)	85.96%	84.21%
	Malignancy	8 (8.42%)	32 (33.68%)	14 (14.74%)		
	Total	57 (60.00%)	38 (40.00%)	95 (100.00%)		

Table 4 Comparison of General Information Between Two Groups ($\bar{x} \pm s$)

Indicators		The Training Group (n=66)	The Validation Group (n=29)	t/χ^2	P
Age		48.52±7.42	49.78±11.05		
BMI		22.05±1.75	22.91±2.87		
Mass size		1.13±0.14	1.20±0.51		
Menstrual condition	menopause	38 (57.58)	19 (65.52)	0.529	0.467
	Premenopausal	28 (42.42)	10 (34.48)		
Education level	Primary school and below	20 (30.30)	13 (44.83)		
	Middle school and vocational school	46 (69.70)	16 (55.17)		
	Bachelor's degree or above	22 (33.33)	12 (41.38)	0.573	0.751
Marital status	First marriage	28 (42.42)	11 (37.93)		
	remarriage	16 (24.24)	6 (20.69)		
	Divorce	40 (60.61)	24 (82.76)	4.924	0.177
	Widow	12 (18.18)	2 (6.90)		
Smoking		8 (12.12)	1 (3.45)		
Drinking		6 (9.09)	2 (6.90)		
Age of initial menstrual period		16 (24.24)	8 (27.59)	0.119	0.730
Delivery situation	Yes	8 (12.12)	5 (17.24)	0.447	0.504
	No	13.01±2.42	12.98±1.35		
Family history of breast cancer		48 (72.73)	23 (79.31)	0.462	0.496
Age		18 (27.27)	6 (20.69)		
BMI		16 (24.24)	8 (27.59)	0.119	0.730

in the training group patients to extract morphological features, first-order features, and texture features. The representative MRI images of the training and validation group were shown in Figure 2A–D. The specific radio-omics parameters were shown in Table 5.

The Value of a Single MRI Parameter in the Diagnosis of Breast Cancer

The SVM classifier was used to construct the imaging model for diagnosis of breast cancer based on the T1WI, T2WI, DWI, ADC, and DCE of patients in the training group. ROC curve analysis showed that the AUC of T1WI, T2WI, DWI, ADC, and DCE in diagnosis of breast cancer were 0.715, 0.769, 0.785, 0.835, and 0.792, respectively (Table 6 and Figure 3).

Value of Combined MRI Parameter in the Diagnosis of Breast Cancer

The SVM classifier was used to construct a multimodal imaging model for diagnosis of breast cancer based on the histological indicators of plain scan (T1WI, T2WI), diffusion (DWI, ADC), and enhancement (DCE) of patients in the training group. ROC curve analysis found that AUC of plain scan, diffuse, enhanced, plain scan + diffuse, plain scan + enhanced, enhanced + diffuse, plain scan + enhanced + diffuse diagnosis of breast cancer was 0.746, 0.798, 0.816, 0.839, 0.890, 0.906, 0.927 respectively (Table 7 and Figure 4).

Discussion

At present, the main imaging methods for clinical diagnosis of breast cancer include ultrasound, X-ray photography, and MRI. Ultrasound is widely used in the screening of breast cancer, but it is difficult to find lesions with small characterization due to the subjective influence of the examiner. X-ray photography is a common examination method in clinical diagnosis, which can be used to diagnose breast cancer by reflecting the size, shape, and microcalcification of the focus tissue. However, X-ray photography is more susceptible to female breast fat, and the cancer diagnostic performance of women who have dense breasts is low.[12] MRI radio-omics utilizes analysis techniques such as texture

**Table 5** Radio-Omics Parameters Related to Lesions

Test mode	Total Number of Features	Morphological Features	First-order Features	Texture Features
Plain scan	107×5 sequence	Flatness, long axis length, diameter slice, elongation, 2D diameter column, 2D diameter slice, 3D diameter, short axis length, surface area, sphericity, grid volume, surface area ratio, voxel volume, minimum axis length, a total of 14 items	Energy, kurtosis, mean absolute deviation, skewness, variance, entropy, maximum, root mean square, total energy, robust mean absolute deviation, median, mean, 10%, 90%, minimum, range, uniformity, quartile range, totaling 18 items	14 GLDM features, 16 GLSZM features, 24 GLCM features, 16 GLRLM features, and 5 NGTDM features, totaling 75 items
Diffusion	109×3 sequence	Flatness, long axis length, diameter slice, elongation, 2D diameter column, 2D diameter slice, 3D diameter, short axis length, surface area, sphericity, grid volume, surface area ratio, voxel volume, minimum axis length, a total of 14 items	75%, energy, kurtosis, mean absolute deviation, skewness, variance, entropy, maximum, root mean square, total energy, robust mean absolute deviation, median, mean, 10%, 90%, minimum, range, uniformity, quartile range, 25%, totaling 20 items	14 GLDM features, 16 GLSZM features, 24 GLCM features, 16 GLRLM features, and 5 NGTDM features, totaling 75 items
Enhancement	107×5 sequence	Flatness, long axis length, diameter slice, elongation, 2D diameter column, 2D diameter slice, 3D diameter, short axis length, surface area, sphericity, grid volume, surface area ratio, voxel volume, minimum axis length, a total of 14 items	Energy, kurtosis, mean absolute deviation, skewness, variance, entropy, maximum, root mean square, total energy, robust mean absolute deviation, median, mean, 10%, 90%, minimum, range, uniformity, quartile range, totaling 18 items	14 GLDM features, 16 GLSZM features, 24 GLCM features, 16 GLRLM features, and 5 NGTDM features, totaling 75 items

Table 6 The Value of a Single MRI in the Diagnosis of Breast Cancer

Indicators	AUC	Accuracy	Sensitivity	Sensitivity
T1WI	0.715	70.16%	75.64%	71.59%
T2WI	0.769	73.96%	71.42%	78.06%
ADC	0.785	74.46%	74.15%	80.12%
DCE	0.835	81.35%	81.01%	86.43%
DWI	0.792	876.13%	83.66%	81.49%

analysis and wavelet analysis to transform the information and features contained in MR images into quantifiable data. In traditional clinical environments, radiologists visually evaluate tumors to obtain tumor morphology and hemodynamic features and make diagnostic decisions. The characteristics of malignant lesions are usually irregular edges, burrs, rapid outflow, uneven internal enhancement, and edge-enhanced lesions.[8] The characteristics of benign lesions are smooth or quasi-circular edges, internal enhancement, uniform enhancement, non-enhanced internal separation, and type of contrast inflow. These features are not always visually distinguishable as they may overlap between two types of lesions. The main objective of radiomics is to extract and quantitatively evaluate hidden information in images that is not visible to the human eye, while eliminating observer bias related to manual examination.[13] DCE is currently the most commonly used MRI technique for diagnosing breast diseases, which distinguishes benign and malignant breast lesions by analyzing high-resolution morphological and hemodynamic changes of breast lesions.[14,15] DWI is a widely used non-invasive MRI examination method in clinical practice without contrast injection. The benign and malignant breast diseases are determined by analyzing the diffusion changes of water molecules in histiocyte and structures. Because of its high
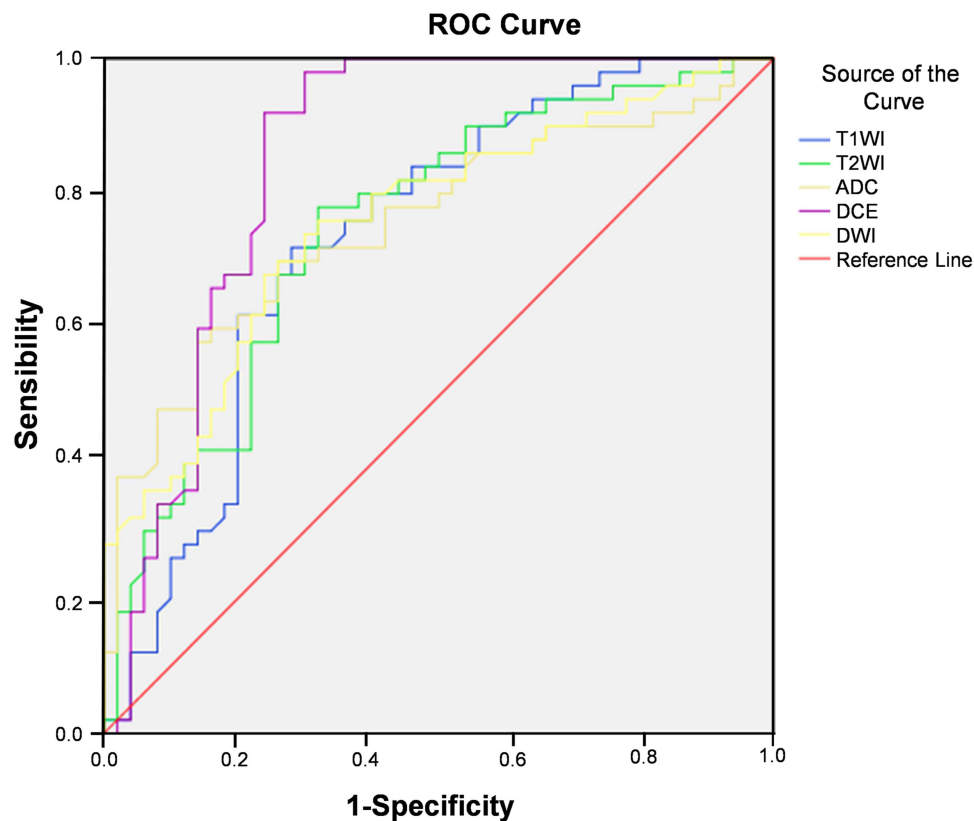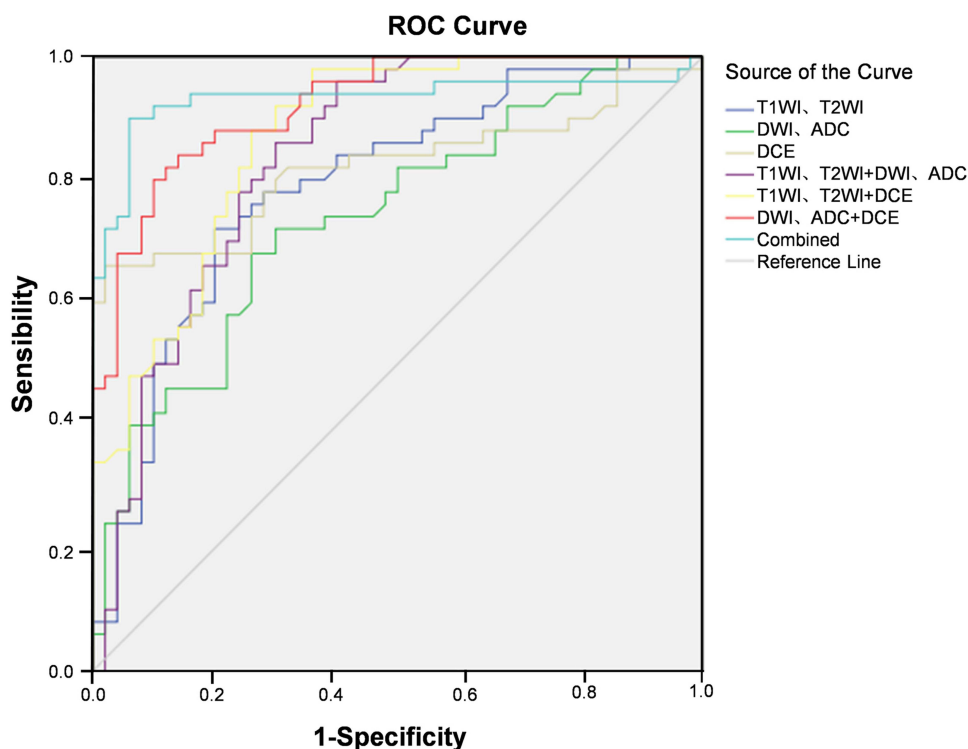
ROC Curve

Figure 3 ROC curve was used to analyze the diagnostic value of radiomics indicators of T1WI, T2WI, DWI, ADC and DCE in breast cancer.

specificity, DWI has become one of the common means for screening breast cancer.[16,17] ADC plot is an apparent diffusion coefficient plot obtained by fitting the diffusion changes of water molecules in DWI with a single index, which can reflect the range of random movement of water molecules in the microstructure of lesion tissue per unit time. ADC maps have important value in diagnosing malignant tumors and differentiating tumor grading.[18,19] In this experiment, the sensitivity of T1WI, T2WI, DWI, ADC and DCE in the diagnosis of breast cancer was 61.14%, 66.67%, 73.30%, 78.95%, and 85.96%. These above results suggested that combined MRI information had certain value in the diagnosis of breast cancer, among which DCE had a high value, which was similar to the research results of Kurihara H et al.[20] Some scholars have established a radiomics model based on DCE-MRI, and it has been found that this model has the potential to predict the efficacy of neoadjuvant chemotherapy for breast cancer.[21] Some partial breast MRI studies mainly extract features from DWI and DCE-MRI images for analysis, without considering T1WI or T2WI.[22,23] Roy et al[24] confirm the importance of TIWI and T2WI in radiomics research. Therefore, each modality image should be considered during the study. Zhang[25] selects 22 radiomics features to construct the SVM model by lasso algorithm, and finds that 6 features

Table 7 Value of Combined MRI in Diagnosis of Breast Cancer

Indicators	AUC	Accuracy	Sensitivity	Sensitivity
Plain scan	0.746	70.18%	76.85%	78.00%
Diffusion	0.798	76.93%	82.59%	83.00%
Enhancement	0.816	78.52%	83.10%	85.74%
Plain scan + diffuse	0.839	80.33%	86.45%	84.15%
Plain scan + enhanced	0.890	85.12%	90.15%	92.05%
Enhanced + diffuse	0.906	86.31%	92.85%	93.00%
Plain scan + enhanced + diffuse	0.927	90.15	96.31%	95.48%

ROC Curve

Figure 4 ROC curve was used to analyze the value of multimodal MRI in the diagnosis of breast cancer.

have no statistical difference after comparing these features between the two groups. Although the clinical significance of these radiomics features is difficult to interpret at present, they still have value in the process of machine learning.

In recent years, with the rapid development of functional imaging technology and image acquisition technology, radio-omics has emerged. Radio-omics improves image analysis by automatically extracting a large number of quantitative features from images with high throughput, including collecting and reconstructing images, segmenting and recombining images, extracting and filtering features, establishing databases, and sharing datasets to construct models. Radio-omics has become an emerging method for imaging diagnosis of diseases.[26] Some scholars[27] respectively used XGBoost and random forest to construct a risk prediction model for premenopausal/postmenopausal breast cancer, screen breast cancer related risk factors and rank them in importance. The top 10 risk factors list of breast cancer screened by the two algorithms shows that the main risk factors before and after menopause include total lactation time, cumulative use time of artificial contraceptive devices, polygenic risk scores (PRS), years of passive smoking, body mass index (BMI), weight information and age. Both models had AUC values greater than 70% before and after menopause. Some scholars used LightGBM model to fully fit target training to reduce model deviation and avoid overfitting, and compared it with XGBoost method. The experimental results showed that LightGBM algorithm had better classification effect, faster training speed and lower memory occupation for the feature vectors in this experiment. Thus, LightGBM model was expected to better assist doctors in diagnosis of breast cancer, improve accuracy and reduce misdiagnosis rate.[28] SVM is a Linear classifier, which can find the separation hyperplane by transforming the classification problem, maximize the realization of classification, and has the maximum possible margin. It is widely used in clinical construction of omics models.[29] Previous studies[30] have shown that adding diffusion and kurtosis to DCE imaging data centers can improve diagnostic efficiency. T2WI and DKI are effective auxiliary sequences for improving the diagnostic efficiency of DCE-MRI. Models based on T1WI or ADC images exhibit lower diagnostic efficiency compared to other single sequence models. Adding the features of T1WI or ADC images to other models does not improve diagnostic performance, possibly due to the contribution of T1WI or ADC to the differential diagnosis of benign and malignant lesions. In this experiment, patients were divided into a training group and a validation group. Morphological features, first-order features, and texture features were extracted from the ROI area of the lesion in the training group through MRI examinations such as

plain scan, diffusion, and enhancement. In order to further analyze the value of MRI imaging model in the diagnosis of breast cancer, ROC curve analysis was established in this experiment. The AUC results suggested that MRI radio-omics model had a certain predictive value in the diagnosis of breast cancer. Among them, the multimodal MRI radio-omics model had a higher predictive value than the single radio-omics model, which could help physicians to early diagnose breast cancer and give effective targeted treatment, and had important significance in improving the prognosis of patients. Different tissue comparisons provide specific representations of tissues and images based on physiological attributes and physics of each tissue type, and the integration of all imaging information from different radiation parameters provides a more complete view of potential biological tissue characteristics. Fusco et al[31] used dynamic, morphological and texture features to classify breast lesions in DCE-MRI, respectively, and compared the performance of five different machine learning algorithms according to the above features. The final results showed that the performance of tree-based classifier was better than that of artificial neural network, support vector machine and Bayesian classifier. Some scholars[32] combined the features of mammography and DCE-MRI to identify benign and malignant non-palpable breast lesions, and the AUC of the classification model constructed by RF reached 0.903. Therefore, combined with the results of other scholars and this study, it can be seen that RF is an effective prediction tool.

The importance of multimodal MRI radiomics: (1) Improvement of the accuracy of early diagnosis of breast cancer. Multimodal MRI radiomics combines a variety of MRI imaging techniques, such as T1WI, T2WI, DCE, etc., which can comprehensively and in detail display the structure, function and metabolism of breast tissue. Comprehensive analysis of these multi-dimensional data will help to improve the detection rate and diagnostic accuracy of early breast cancer. (2) Development of individualized treatment regimens. Multi-modality MRI radiomics can provide rich biomarker information, such as tumor size, shape, margin, and hemodynamic characteristics, which is helpful to more accurately evaluate the biological behavior and prognosis of breast cancer. This information is essential for the development of an individualized treatment plan, which can help physicians to choose the most appropriate treatment method, improve the treatment effect, and reduce the recurrence rate.

Economic benefit analysis: (1) By reducing unnecessary medical expenses, early diagnosis can significantly improve the survival rate of breast cancer patients, and reduce the complexity and high cost of late treatment. The application of multimodal MRI radiomics can detect breast cancer at an early stage, thereby reducing unnecessary medical expenses and the economic burden on society and individuals. (2) Promoting the development of the medical industry. With the promotion and application of multimodal MRI radiomics technology, it will promote the development of related medical devices, diagnostic reagents, data processing software and other industries. This will not only create new economic growth points for the medical industry, but also help to promote the progress of the whole medical technology, forming a virtuous circle.

Multimodal MRI radiomics can more accurately identify and evaluate the disease of breast cancer patients by combining a variety of imaging techniques. This allows many patients to be diagnosed at an earlier stage, resulting in improved treatment outcomes and survival rates. However, while this technology brings benefits, it also exposes some ethical issues. First, for the protection of patient privacy, multi-modality MRI radiomics needs to collect a large amount of patient personal information, including biological characteristics, genetic information, etc. Disclosure of such information could lead to violation of patient privacy rights. Therefore, in the process of data collection, storage and use, medical institutions and relevant researchers should strictly abide by the principle of privacy protection to ensure the security of patient information.

Comparison of the advantages of multimodal MRI radiomics with other diagnostic methods: Compared with traditional imaging, multimodal MRI radiomics has obvious advantages in spatial resolution and tissue specificity. It can more accurately display the biological characteristics of tumors and provide more accurate diagnostic information for clinicians. Compared with biomarker detection, multimodal MRI radiomics can obtain rich biomarker information without invasive operation. In addition, it can also monitor the biological changes of tumors in real time, providing a strong basis for clinical treatment. Compared with genetic testing, multimodal MRI radiomics has the advantages of non-invasive, rapid and low cost. Although genetic testing is of great value in the diagnosis of breast cancer, multi-modal MRI radiomics can make up for the deficiency of genetic testing to a certain extent and provide more information for clinical decision-making.

Conclusion

To sum up, the construction of radio-omics models based on the quantitative characteristics of multimodal MRI images had a certain value in the diagnosis of breast cancer. Among them, combined radio-omics models such as plain scan + enhanced + diffuse had a higher value in the diagnosis of breast cancer and could be widely used in clinical practice. However, due to the short study time, small sample size, and only extracting the radiomics features within the tumor without adding the radiomics features around the tumor, the experimental results may have a contingency and cannot truly reflect the performance of the model to a certain extent. In addition, to facilitate image processing, only patients with mass lesions were included in the study, and patients with non-mass enhancement were not analyzed. In this study, only radiomics features were used to establish a model, and other clinical and genetic factors were not combined for comprehensive analysis. In the future, the experimental objects and research time will be expanded, and the research on the progress of radio-omics characteristics of the tissues around the tumor will be carried out.

Research innovation: Highly personalized: Multimodal MRI radiomics can achieve highly personalized diagnosis according to individual differences of patients. By analyzing the MRI features of different patients, the tailored diagnostic scheme was developed to improve the diagnostic accuracy. Application of deep learning technology: Deep learning technology is applied to multimodal MRI radiomics to achieve automatic extraction, classification and recognition of image data, and greatly improve the efficiency of diagnosis. In addition, deep learning technology can also find small myocardial infarction foci that are difficult to be identified by traditional imaging, which provides strong support for early diagnosis. Multi-parameter joint analysis: Multimodal MRI radiomics can comprehensively evaluate the biological characteristics of breast cancer by jointly analyzing a variety of imaging parameters, such as morphological, functional and metabolic parameters, and provide powerful guidance for clinical treatment. Artificial intelligence-assisted diagnosis: Combined with artificial intelligence technology, multimodal MRI radiomics can achieve rapid and accurate diagnosis of breast cancer, reduce the workload of doctors, and improve the efficiency of diagnosis.

Future perspectives: Data mining: Multi-modal MRI radiomics data were further mined to find more characteristic parameters with diagnostic value and improve the accuracy of breast cancer diagnosis. Interdisciplinary research: Strengthen multidisciplinary cooperation, such as biology, pathology, genetics, etc. to comprehensively reveal the pathogenesis of breast cancer and provide new ideas for diagnosis and treatment. Individualized treatment: To develop individualized treatment plans based on multimodal MRI radiomics features to achieve precision medicine. Optimization of artificial intelligence technology: The artificial intelligence algorithm was continuously optimized to improve the performance of multimodal MRI radiomics in breast cancer diagnosis.

Data Sharing Statement

The datasets used and/or analyzed during the current study are available from the corresponding author on reasonable request.

Ethics Approval and Consent to Participate

This study was approved by The Ethics Committee of Fujian Maternity and Child Health Hospital. Informed consent was obtained from participants for the participation in the study and all methods were carried out in accordance with relevant guidelines and regulations.

Author Contributions

All authors made a significant contribution to the work reported, whether that is in the conception, study design, execution, acquisition of data, analysis and interpretation, or in all these areas; took part in drafting, revising or critically reviewing the article; gave final approval of the version to be published; have agreed on the journal to which the article has been submitted; and agree to be accountable for all aspects of the work.

Disclosure

The authors declare that they have no competing interests.

References

1. Riggio AI, Varley KE, Welm AL. The lingering mysteries of metastatic recurrence in breast cancer. *Br J Cancer*. 2021;124(1):13–26. doi:10.1038/s41416-020-01161-4

2. Bray F, Ferlay J, Soerjomataram I, Siegel RL, Torre LA, Jemal A. Global cancer statistics 2018: GLOBOCAN estimates of incidence and mortality worldwide for 36 cancers in 185 countries. *CA Cancer J Clin*. 2018;68(6):394–424. doi:10.3322/caac.21492

3. Fumoleau P, Roché H, Kerbrat P, et al; French Adjuvant Study Group. Long-term cardiac toxicity after adjuvant epirubicin-based chemotherapy in early breast cancer: French results. *Ann Oncol*. 2006;17(1):85–92. doi:10.1093/annonc/mdj034

4. Wang J, Sun T, Ouyang Q, Han Y, Xu B. A phase Ib study of TQB2450 plus anlotinib in patients with advanced triple-negative breast cancer. *iScience*. 2023;26(6):106876. doi:10.1016/j.isci.2023.106876

5. Sumkin JH, Berg WA, Carter GJ, et al. Diagnostic performance of MRI, molecular breast imaging, and contrast-enhanced mammography in women with newly diagnosed breast cancer. *Radiology*. 2019;293(3):531–540. doi:10.1148/radiol.2019190887

6. Hollingsworth AB, Pearce MR, Stough RG. Breast cancer survival following MRI detection in a high-risk screening program. *Breast J*. 2020;26(5):991–994. doi:10.1111/tbj.13813

7. Marshall H, Pham R, Sieck L, Plecha D. Implementing abbreviated MRI screening into a breast imaging practice. *AJR Am J Roentgenol*. 2019;213(1):234–237. doi:10.2214/AJR.18.20396

8. Cui Q, Sun L, Zhang Y, et al. Value of breast MRI omics features and clinical characteristics in Breast Imaging Reporting and Data System (BI-RADS) category 4 breast lesions: an analysis of radiomics-based diagnosis. *Ann Transl Med*. 2021;9(22):1677. doi:10.21037/atm-21-5441

9. Upadhaya T, Morin O, Park CC. Second-harmonic generation image based histomics for the prediction of breast cancer recurrence. *Int J Radiat Oncol Biol Phys*. 2020;108(3):e70–e71. doi:10.1016/j.ijrobp.2020.07.1144

10. Li Q, Luo Y, Liu D, Li B, Liu Y, Wang T. Construction and prognostic value of enhanced CT image omics model for noninvasive prediction of HRG in bladder cancer based on logistic regression and support vector machine algorithm. *Front Oncol*. 2023;12:966506. doi:10.3389/fonc.2022.966506

11. LoGullo R, Horvat J, Reiner J, Pinker K. Multimodale, parametrische und genetische brustbildgebung [Multimodal, multiparametric and genetic breast imaging]. *Radiologe*. 2021;61(2):183–191. doi:10.1007/s00117-020-00801-3

12. Zaric O, Farr A, Poblador Rodriguez E, et al. 7T CEST MRI: a potential imaging tool for the assessment of tumor grade and cell proliferation in breast cancer. *Magn Reson Imaging*. 2019;59:77–87. doi:10.1016/j.mri.2019.03.004

13. Wang X, Wang X, Zhang Y, et al. Development of the prediction model based on clinical-imaging omics: molecular typing and sentinel lymph node metastasis of breast cancer. *Ann Transl Med*. 2022;10(13):749. doi:10.21037/atm-22-2844

14. Heacock L, Lewin AA, Toth HK, Moy L, Reig B. Abbreviated MR imaging for breast cancer. *Radiol Clin North Am*. 2021;59(1):99–111. pii: S0033-8389(20)30115-9. doi:10.1016/j.rcl.2020.09.001

15. Grubstein A, Rapson Y, Stemmer SM, et al. Timing to imaging and surgery after neoadjuvant therapy for breast cancer. *Clin Imaging*. 2021;71:24–28. doi:10.1016/j.clinimag.2020.10.043

16. Carmona-Bozo JC, Manavaki R, Woitek R, et al. Hypoxia and perfusion in breast cancer: simultaneous assessment using PET/MR imaging. *Eur Radiol*. 2021;31(1):333–344. doi:10.1007/s00330-020-07067-2

17. Pujara AC, Kim E, Axelrod D, Melsaether AN. PET/MRI in Breast Cancer. *J Magn Reson Imaging*. 2019;49(2):328–342. doi:10.1002/jmri.26298

18. Partovi S, Sin D, Lu Z, et al. Fast MRI breast cancer screening - Ready for prime time. *Clin Imaging*. 2020;60(2):160–168. doi:10.1016/j.clinimag.2019.10.013

19. Sorace AG, Virostko J, Wu C, et al. Abstract P1-01-02: quantitative breast MRI to predict response to neoadjuvant therapy in community imaging centers: preliminary results. *Cancer Res*. 2019;79(4 Supplement):P1-01-02-P1-01-02. doi:10.1158/1538-7445.SABCS18-P1-01-02

20. Kurihara H, Shimizu C, Miyakita Y, et al. Molecular imaging using PET for breast cancer. *Breast Cancer*. 2016;23(1):24–32. doi:10.1007/s12282-015-0613-z

21. Montemezzi S, Benetti G, Bisighin MV, et al. 3T DCE-MRI radiomics improves predictive models of complete response to neoadjuvant chemotherapy in breast cancer. *Front Oncol*. 2021;11:630780. doi:10.3389/fonc.2021.630780

22. Ma M, Gan L, Jiang Y, et al. Radiomics analysis based on automatic image segmentation of DCE-MRI for predicting triple-negative and nontriple-negative breast cancer. *Comput Math Methods Med*. 2021;2021:2140465. doi:10.1155/2021/2140465

23. Qi X, Wang W, Pan S, et al. Predictive value of triple negative breast cancer based on DCE-MRI multi-phase full-volume ROI clinical radiomics model. *Acta Radiol*. 2024;65(2):173–184. doi:10.1177/02841851231215145

24. Roy S, Whitehead TD, Quirk JD, et al. Optimal co-clinical radiomics: sensitivity of radiomic features to tumour volume, image noise and resolution in co-clinical T1-weighted and T2-weighted magnetic resonance imaging. *EBioMedicine*. 2020;59:102963. doi:10.1016/j.ebiom.2020.102963

25. Zhang Q, Peng Y, Liu W, et al. Radi omics based on multimodal MRI for the Di fferential Di agnosis of B enign and M alignant breast lesi ons. *J Magn Reson Imaging*. 2020;52(2):596–607. doi:10.1002/jmri.27098

26. Latini F, Fahlström M, Fällmar D, Marklund N, Cunningham JL, Feresiadou A. Can diffusion tensor imaging (DTI) outperform standard magnetic resonance imaging (MRI) investigations in post-COVID-19 autoimmune encephalitis? *Ups J Med Sci*. 2022;127. doi:10.48101/ujms.v127.8562

27. Li Q, Yang H, Wang P, Liu X, Lv K, Ye M. XGBoost-based and tumor-immune characterized gene signature for the prediction of metastatic status in breast cancer. *J Transl Med*. 2022;20(1):177. doi:10.1186/s12967-022-03369-9

28. Pan J, Ma B, Hou X, et al. The construction of transcriptional risk scores for breast cancer based on lightGBM and multiple omics data. *Math Biosci Eng*. 2022;19(12):12353–12370. doi:10.3934/mbe.2022576

29. Tong L, Wu H, Wang MD. Integrating multi-omics data by learning modality invariant representations for improved prediction of overall survival of cancer. *Methods*. 2021;189:74–85. doi:10.1016/j.ymeth.2020.07.008

30. Sun SY, Ding Y, Li Z, et al. Multiparameter MRI Model With DCE-MRI, DWI, and Synthetic MRI Improves the Diagnostic Performance of BI-RADS 4 Lesions. *Front Oncol*. 2021;11:699127. doi:10.3389/fonc.2021.699127

31. Fusco R, Sansone M, Filice S, et al. Pattern recognition approaches for breast cancer DCE-MRI classification: a systematic review. *J Med Biol Eng*. 2016;36(4):449–459. doi:10.1007/s40846-016-0163-7

32. Zhao YF, Chen Z, Zhang Y, et al. Diagnosis of breast cancer using radiomics models built based on dynamic contrast enhanced MRI combined with mammography. *Front Oncol*. 2021;11:774248. doi:10.3389/fonc.2021.774248